# Analysis of Rectangular Waveguide Junctions by the Method of Lines

Wilfrid Pascher, *Member, IEEE*, and Reinhold Pregla, *Senior Member, IEEE*

*Abstract*— **A novel discretization on two crossed line systems is introduced in the method of lines to analyze junctions in rectangular waveguides. This discretization is one-dimensional and replaces the two-dimensional discretization otherwise necessary for such structures. Hence the matrices encountered are small compared with other approaches. Equivalent circuits for the right-angle $E$-plane corner and scattering parameters for the asymmetric T-junction are presented, which agree very well with literature.**

## I. Introduction

THE MODE matching technique is the classical method for the analysis of junctions in rectangular waveguides [1]–[3]. By the method of lines (MoL) [4], [5], a variety of planar and dielectric waveguide structures has been investigated (for a comprehensive description see [6]). It has also been applied to discontinuities in rectangular waveguides [5], [7]–[9].

In this paper the MoL is adapted for the efficient analysis of junctions in rectangular waveguides. For its application to $E$-plane or $H$-plane junctions (Fig. 1), we use the known field behavior in one transverse direction and discretize the wave equation in the other transverse direction only [8]. In order to avoid two-dimensional discretization normally necessary for waveguide junctions, a novel approach is introduced, where the potential and the fields are evaluated on two line systems perpendicular to each other. Each line system represents a one-dimensional discretization as it is used to model, for example, a step discontinuity yielding two independent solutions of the wave equation. Additionally, the potential at the interfaces between different waveguide regions (Fig. 2) is suitably matched. Finally, the generalized scattering matrix is computed. Cascaded junctions are analyzed by combining the matrices relating the incoming and outgoing waves.

In the following, the approach is applied to various $E$-plane junctions. Equivalent circuits for the right-angle corner and scattering parameters for the asymmetric T-junction are presented. A generalization to $H$-plane structures is straightforward.

## II. Crossed Line Systems for the Analysis of Waveguide Junctions

Generally, junctions in rectangular waveguides, as in Fig. 2, are divided into the waveguide regions $i$ ($i = 1, \ldots, 4$) and

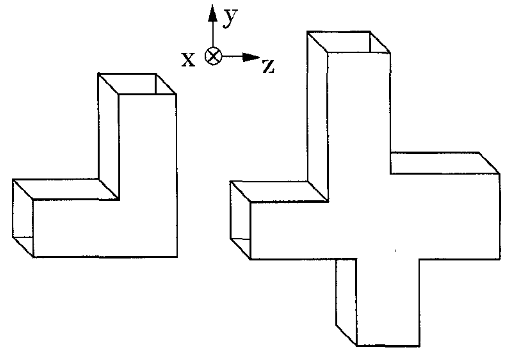


Fig. 1. Junctions in rectangular waveguides.

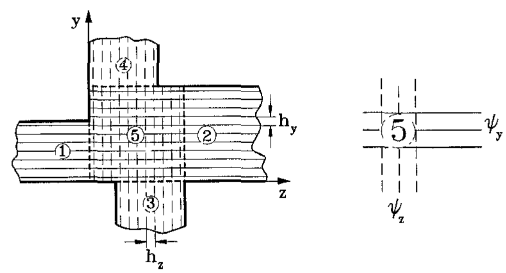


Fig. 2. Discretization of a waveguide junction on two crossed line systems.

the resonator region 5, similar to the resonator method after Kühn [1]. In case of a two port consisting of the regions 1 and 2 only, the problem is reduced to the analysis of discontinuities, as presented in [8]. The procedure described in this section employs the novel approach of the two crossed line systems (Fig. 2) to extend the method for the investigation of multiports. In what follows, formulas already developed for discontinuities are only summarized, and the reader is referred to [8] for a more comprehensive derivation.

For $TE_{1n}$-to-$x$ modes, which are the only modes arising from the junctions of Fig. 1 by excitation with $TE_{10}$-to-$x$ waves, the electromagnetic fields in all five regions are derived from the potential $\psi$ by

$$\begin{aligned} E_x &= 0 & \eta_0 H_x &= (\varepsilon_r - \overline{\lambda}_x^2) \sin \overline{\lambda}_x \overline{x} \cdot \psi \\ E_y &= -j \sin \overline{\lambda}_x \overline{x} \cdot \frac{\partial \psi}{\partial \overline{z}} & \eta_0 H_y &= \overline{\lambda}_x \cos \overline{\lambda}_x \overline{x} \cdot \frac{\partial \psi}{\partial \overline{y}} \\ E_z &= j \sin \overline{\lambda}_x \overline{x} \cdot \frac{\partial \psi}{\partial \overline{y}} & \eta_0 H_z &= \overline{\lambda}_x \cos \overline{\lambda}_x \overline{x} \cdot \frac{\partial \psi}{\partial \overline{z}} \end{aligned} \quad (1)$$

with a time dependence $\exp(j\omega t)$ and $\overline{\lambda}_x = \pi/\overline{a}$. The waveguide width $a$ is assumed to be constant for the whole structure, and all lengths are normalized by $\overline{x} = k_0 x$, etc. The

Manuscript received June 2, 1994; revised August 29, 1995. This work was supported by the Deutsche Forschungsgemeinschaft.

The authors are with Allgemeine und Theoretische Elektrotechnik, FernUniversität, D-58084 Hagen, Germany.

IEEE Log Number 9415555.

0018–9480/95$04.00 © 1995 IEEE

potential $\psi$ must fulfill the Neumann condition at all metallic boundaries.

### A. Discretization and Transformed Potentials

In the resonator region 5, the potential $\boldsymbol{\psi}$ is discretized on *two crossed line systems* running in $z$ and $y$ direction, as shown in Fig. 2, such that the potential is decomposed into two parts

$$\boldsymbol{\psi} = \boldsymbol{\psi}_y + \boldsymbol{\psi}_z. \tag{2}$$

$\boldsymbol{\psi}_y$ is defined on the horizontal lines and corresponds to the $\boldsymbol{\psi}$ for the step discontinuity, whereas $\boldsymbol{\psi}_z$ is defined on the vertical lines and fulfills the Neumann condition on the left and right boundary.

As in [8], we discretize the Helmholtz equation

$$\frac{\partial^2\psi}{\partial\overline{z}^2} + \frac{\partial^2\psi}{\partial\overline{y}^2} - \overline{\lambda}_x^2\psi + \varepsilon_r\psi = 0 \tag{3}$$

but separately for $\boldsymbol{\psi}_y$ and $\boldsymbol{\psi}_z$ and obtain, for example, for the potential $\boldsymbol{\psi}_z$

$$\frac{d^2\boldsymbol{\psi}_z}{d\overline{y}^2} - \left(-(\overline{\mathrm{h}}_z)^{-2}\boldsymbol{D}_{zz} + (\overline{\lambda}_x^2 - \varepsilon_r)\boldsymbol{I}\right)\boldsymbol{\psi}_z = \mathbf{0}. \tag{4}$$

The difference operator $\boldsymbol{D}_{zz}$ is transformed to principal axes by

$$(\overline{\mathrm{h}}_z)^{-2}\,\boldsymbol{T}_z^t\boldsymbol{D}_{zz}\boldsymbol{T}_z = -\overline{\boldsymbol{\lambda}}_z^2. \tag{5}$$

We obtain the general solution for the transformed potential

$$\overline{\boldsymbol{\psi}}_z = \boldsymbol{T}_z^t\boldsymbol{\psi}_z = \exp(-\boldsymbol{\Gamma}_y\overline{y})\boldsymbol{A}_z + \exp(\boldsymbol{\Gamma}_y\overline{y})\,\mathbf{B}_z \tag{6}$$

with the diagonal propagation matrix in $y$ direction

$$\boldsymbol{\Gamma}_y = \mathrm{diag}\,(\gamma_{yk}) = \left(\overline{\boldsymbol{\lambda}}_z^2 + (\overline{\lambda}_x^2 - \varepsilon_r)\boldsymbol{I}\right)^{\frac{1}{2}}. \tag{7}$$

For the two potentials $\boldsymbol{\psi}_y$ and $\boldsymbol{\psi}_z$, two different kinds of discretization distances $\mathrm{h}_{y,z}$, line numbers $N_{y,z}$, transformation matrices $\boldsymbol{T}_{y,z}$, wave vectors $\mathbf{A}_{y,z}$, $\mathbf{B}_{y,z}$, and propagation matices $\boldsymbol{\Gamma}_{y,z}$ are introduced in the resonator region 5 where, for example, $\boldsymbol{T}_y$ is the transformation matrix for $\boldsymbol{\psi}_y$. Only $\boldsymbol{\Gamma}_y$ belongs to $\boldsymbol{\psi}_z$ because it stands for the propagation in $y$ direction. The waveguide region $i$ is treated as for the step discontinuity with the according potentials $\boldsymbol{\psi}_i$, and the quantities $N_i$, $\boldsymbol{T}_i$, $\mathbf{A}_i$, $\mathbf{B}_i$, and $\boldsymbol{\Gamma}_i$ belonging to it.

### B. Field Matching at the Terminal Planes

We have to match the transverse electromagnetic field at each terminal plane $i$, which is the interface between waveguide $i$ and the resonator region 5. First we establish the matching equations at terminal 1. Here $E_y$ and $H_x$, that means $\psi$ and $\partial\psi/\partial\overline{z}$, must be matched. If $\psi$ is matched on all the discretization lines, $\partial\psi/\partial\overline{y}$ and thus $H_y$ is also matched.

For the *derivative* of the first potential $\partial\boldsymbol{\psi}_y/\partial\overline{z}$ we obtain a completely analogous equation as for the step discontinuity since the derivative of the second potential $\partial\boldsymbol{\psi}_z/\partial\overline{z}$ vanishes because of the Neumann condition

$$\boldsymbol{R}_1\,(\mathbf{A}_1 - \mathbf{B}_1) = \mathbf{A}_y - \mathbf{B}_y \tag{8}$$

with

$$\boldsymbol{R}_1 = \boldsymbol{\Gamma}_z^{-1}\boldsymbol{T}_{y\to1}^t\boldsymbol{T}_1\boldsymbol{\Gamma}_1$$

where $\boldsymbol{T}_{y\to1}$ is an $N_1 \times N_y$ matrix which consists of those elements of $\boldsymbol{T}_y$ corresponding to the common aperture of regions 1 and 5.

So far the analysis was equal to that for the step discontinuity [8]. For the matching of the potential $\boldsymbol{\psi}$ *itself*, however, $\boldsymbol{\psi}_z$ must be considered as an additional term

$$\boldsymbol{T}_1\,(\mathbf{A}_1 + \mathbf{B}_1) = \boldsymbol{T}_{y\to1}\,(\mathbf{A}_y + \mathbf{B}_y) + \underbrace{+\,(\boldsymbol{G}_{z\to1}^{+}\mathbf{A}_z + \boldsymbol{G}_{z\to1}^{-}\mathbf{B}_z)}_{\boldsymbol{\psi}_z} \tag{9}$$

where $\boldsymbol{G}_{z\to1}^{\pm}$ is an $N_1 \times N_z$ matrix, namely the Fourier matrix for extrapolation of $\boldsymbol{\psi}_z$ from region 5 to terminal 1 (see the Appendix)

$$(\boldsymbol{G}_z^{\pm})_{ik} = \sqrt{\frac{2-\delta_{0k}}{N_z}}\exp(\pm\gamma_{yk}\overline{y}_i)\quad(k = 0\ldots N_z - 1). \tag{10}$$

Analogous equations result for terminal 2

$$\boldsymbol{R}_2\,(\mathbf{B}_2 - \mathbf{A}_2) = \boldsymbol{F}_y^{-}\mathbf{A}_y - \boldsymbol{F}_y^{+}\mathbf{B}_y \tag{11}$$

$$\boldsymbol{T}_2\,(\mathbf{B}_2 + \mathbf{A}_2) = \boldsymbol{T}_{y\to2}\,(\boldsymbol{F}_y^{-}\mathbf{A}_y + \boldsymbol{F}_y^{+}\mathbf{B}_y) + \underbrace{+\,(\boldsymbol{G}_{z\to2}^{-}\boldsymbol{V}_z\mathbf{A}_z + \boldsymbol{G}_{z\to2}^{+}\boldsymbol{V}_z\mathbf{B}_z)}_{\boldsymbol{\psi}_z} \tag{12}$$

where the normalized distance $\bar{l}_z$ between terminal 1 and 2 is taken into account by the Fourier matrix $\boldsymbol{F}_y$ and the sign matrix $\boldsymbol{V}_z$ defined by

$$\boldsymbol{F}_y^{\pm} = \exp(\pm\boldsymbol{\Gamma}_z\bar{l}_z)$$
$$\boldsymbol{V}_z = \mathrm{diag}\,((-1)^k)\quad(k = 0\ldots N_z - 1). \tag{13}$$

For terminals 3 and 4, we use (8)–(13) with $y$ and $z$ interchanged.

### C. Determination of the Scattering Matrix

To compute the scattering matrix, we have to establish a relation between the wave vectors $\mathbf{A}_i$ and $\mathbf{B}_i$ by eliminating $\mathbf{A}_y$, $\mathbf{B}_y$ and $\mathbf{A}_z$, $\mathbf{B}_z$ from (8)–(12). First, we calculate the wave vectors $\mathbf{A}_y$, $\mathbf{B}_y$ in region 5 from (8) and (11)

$$\begin{bmatrix}\mathbf{A}_y\\ \mathbf{B}_y\end{bmatrix} = \begin{bmatrix}\boldsymbol{F}_y^{+} & \boldsymbol{I}\\ \boldsymbol{F}_y^{-} & \boldsymbol{I}\end{bmatrix}(\boldsymbol{F}_y^{+} - \boldsymbol{F}_y^{-})^{-1}\begin{bmatrix}\boldsymbol{R}_1\,(\mathbf{A}_1 - \mathbf{B}_1)\\ \boldsymbol{R}_2\,(\mathbf{A}_2 - \mathbf{B}_2)\end{bmatrix}. \tag{14}$$

This equation is valid only for

$$(\boldsymbol{F}_y^{+} - \boldsymbol{F}_y^{-})_i = 2(\sinh\boldsymbol{\Gamma}_z\bar{l}_z)_i \neq 0 \tag{15}$$

that means

$$\bar{l}_z \neq 0 \quad\text{and}\quad -j\gamma_{zi} = k_{zi} \neq n\pi/\bar{l}_z$$

which is the case if no resonance occurs. The wave vectors $\mathbf{A}_z$, $\mathbf{B}_z$ of the potential $\boldsymbol{\psi}_z$ are computed completely analogously from $\mathbf{A}_3$, $\mathbf{B}_3$ and $\mathbf{A}_4$, $\mathbf{B}_4$.

Now we substitute $\mathbf{A}_y$, $\mathbf{B}_y$ and $\mathbf{A}_z$, $\mathbf{B}_z$ into (9) and (12) and thus obtain (16)–(18), shown at the top of the next page. The coupling matrices $\mathcal{G}_i$ must be reduced to the appropriate line

$$\begin{bmatrix} \boldsymbol{T}_1\,(\mathbf{A}_1+\mathbf{B}_1) \\ \boldsymbol{T}_2\,(\mathbf{A}_2+\mathbf{B}_2) \end{bmatrix} = \begin{bmatrix} \boldsymbol{T}_{y\to 1}\,(\tanh \boldsymbol{\Gamma}_z \bar{l}_z)^{-1} & \boldsymbol{T}_{y\to 1}\,(\sinh \boldsymbol{\Gamma}_z \bar{l}_z)^{-1} \\ \boldsymbol{T}_{y\to 2}\,(\sinh \boldsymbol{\Gamma}_z \bar{l}_z)^{-1} & \boldsymbol{T}_{y\to 2}\,(\tanh \boldsymbol{\Gamma}_z \bar{l}_z)^{-1} \end{bmatrix} \begin{bmatrix} \boldsymbol{R}_1\,(\mathbf{A}_1-\mathbf{B}_1) \\ \boldsymbol{R}_2\,(\mathbf{A}_2-\mathbf{B}_2) \end{bmatrix} + \begin{bmatrix} \mathcal{G}_{3\to 1} & \mathcal{G}_{4\to 1} \\ \mathcal{G}_{3\to 2}\boldsymbol{V}_z & \mathcal{G}_{4\to 2}\boldsymbol{V}_z \end{bmatrix} (\sinh \boldsymbol{\Gamma}_y \bar{l}_y)^{-1} \begin{bmatrix} \boldsymbol{R}_3\,(\mathbf{A}_3-\mathbf{B}_3) \\ \boldsymbol{R}_4\,(\mathbf{A}_4-\mathbf{B}_4) \end{bmatrix} \quad (16)$$

with the coupling matrices

$$\begin{aligned} \mathcal{G}_1 &= \tfrac{1}{2}\left(\boldsymbol{G}_y^- \boldsymbol{F}_y^+ + \boldsymbol{G}_y^+ \boldsymbol{F}_y^-\right) & \mathcal{G}_3 &= \tfrac{1}{2}\left(\boldsymbol{G}_z^- \boldsymbol{F}_z^+ + \boldsymbol{G}_z^+ \boldsymbol{F}_z^-\right) \\ \mathcal{G}_2 &= \tfrac{1}{2}\left(\boldsymbol{G}_y^- + \boldsymbol{G}_y^+\right) & \mathcal{G}_4 &= \tfrac{1}{2}\left(\boldsymbol{G}_z^- + \boldsymbol{G}_z^+\right) \end{aligned} \quad (17)$$

namely

$$\begin{aligned} (\mathcal{G}_1)_{ik} &= \sqrt{\tfrac{2-\delta_{0k}}{N_z}}\,\cosh \gamma_{zk}(\bar{l}_z - \bar{z}_i) & (\mathcal{G}_3)_{ik} &= \sqrt{\tfrac{2-\delta_{0k}}{N_y}}\,\cosh \gamma_{yk}(\bar{l}_y - \bar{y}_i) \\ (\mathcal{G}_2)_{ik} &= \sqrt{\tfrac{2-\delta_{0k}}{N_z}}\,\cosh \gamma_{zk}\bar{z}_i & (\mathcal{G}_4)_{ik} &= \sqrt{\tfrac{2-\delta_{0k}}{N_y}}\,\cosh \gamma_{yk}\bar{y}_i \end{aligned} \quad (18)$$

numbers; for example, $\mathcal{G}_{3\to 1}$ is an $N_1 \times N_3$ matrix containing the corresponding elements of $\mathcal{G}_3$. If the terminals in $y$ and $z$ direction are interchanged, that is, $1 \leftrightarrow 3$ and $2 \leftrightarrow 4$, (16) is replaced by a completely analogous one.

For the determination of the **scattering matrix**, we compute the outgoing waves $\mathbf{B}_i$ from the incoming ones $\mathbf{A}_i$ and obtain the desired system of equations

$$\left[\begin{array}{cc|cc} \mathcal{T}_1^+ & \mathcal{T}_{12} & \boldsymbol{W}_{13} & \boldsymbol{W}_{14} \\ \mathcal{T}_{21} & \mathcal{T}_2^+ & \boldsymbol{W}'_{23} & \boldsymbol{W}'_{24} \\ \hline \boldsymbol{W}_{31} & \boldsymbol{W}_{32} & \mathcal{T}_3^+ & \mathcal{T}_{34} \\ \boldsymbol{W}'_{41} & \boldsymbol{W}'_{42} & \mathcal{T}_{43} & \mathcal{T}_4^+ \end{array}\right] \begin{bmatrix} \mathbf{B}_1 \\ \mathbf{B}_2 \\ \mathbf{B}_3 \\ \mathbf{B}_4 \end{bmatrix} = \left[\begin{array}{cc|cc} \mathcal{T}_1^- & \mathcal{T}_{12} & \boldsymbol{W}_{13} & \boldsymbol{W}_{14} \\ \mathcal{T}_{21} & \mathcal{T}_2^- & \boldsymbol{W}'_{23} & \boldsymbol{W}'_{24} \\ \hline \boldsymbol{W}_{31} & \boldsymbol{W}_{32} & \mathcal{T}_3^- & \mathcal{T}_{34} \\ \boldsymbol{W}'_{41} & \boldsymbol{W}'_{42} & \mathcal{T}_{43} & \mathcal{T}_4^- \end{array}\right] \begin{bmatrix} \mathbf{A}_1 \\ \mathbf{A}_2 \\ \mathbf{A}_3 \\ \mathbf{A}_4 \end{bmatrix}. \quad (19)$$

The submatrices of the first two columns are determined as shown in (20) at the bottom of the page. The submatrices of the last two columns ($n = 3, 4$) are obtained changing $y$ to $z$ in (20) and vice versa.

*D. Waveguide Corner*

In the case of the rectangular waveguide corner we can simplify the above results. We delete the second and fourth row and column in (19) and obtain

$$\begin{bmatrix} \mathcal{T}_1^+ & \boldsymbol{W}_{13} \\ \boldsymbol{W}_{31} & \mathcal{T}_3^+ \end{bmatrix} \begin{bmatrix} \mathbf{B}_1 \\ \mathbf{B}_3 \end{bmatrix} = \begin{bmatrix} \mathcal{T}_1^- & \boldsymbol{W}_{13} \\ \boldsymbol{W}_{31} & \mathcal{T}_3^- \end{bmatrix} \begin{bmatrix} \mathbf{A}_1 \\ \mathbf{A}_3 \end{bmatrix}. \quad (21)$$

If we have $N_z = N_1$ and $N_y = N_3$ as in the plain corner, the respective $\boldsymbol{T}$ and $\boldsymbol{\Gamma}$ matrices are equal, namely

$$\begin{aligned} \boldsymbol{T}_y &= \boldsymbol{T}_1 & \boldsymbol{T}_z &= \boldsymbol{T}_3 \\ \boldsymbol{\Gamma}_z &= \boldsymbol{\Gamma}_1 & \boldsymbol{\Gamma}_y &= \boldsymbol{\Gamma}_3 \end{aligned} \quad (22)$$

and hence $\boldsymbol{R}_k = \boldsymbol{I}$, which simplifies the submatrices $\mathcal{T}$ and $\boldsymbol{W}$ in (20) according to, for example

$$\begin{aligned} \mathcal{T}_1^{\pm} &= \boldsymbol{T}_1\,(\pm \boldsymbol{I} + (\tanh \boldsymbol{\Gamma}_z \bar{l}_z)^{-1}) \\ \boldsymbol{W}_{13} &= \mathcal{G}_3\,(\sinh \boldsymbol{\Gamma}_z \bar{l}_z)^{-1}. \end{aligned} \quad (23)$$

We can now rewrite (21) in the form

$$\begin{bmatrix} \boldsymbol{F}_z^+ & \boldsymbol{T}_1^t \mathcal{G}_3 \\ \boldsymbol{T}_3^t \mathcal{G}_1 & \boldsymbol{F}_y^+ \end{bmatrix} \begin{bmatrix} \mathbf{B}'_1 \\ \mathbf{B}'_3 \end{bmatrix} = \begin{bmatrix} \boldsymbol{F}_z^- & \boldsymbol{T}_1^t \mathcal{G}_3 \\ \boldsymbol{T}_3^t \mathcal{G}_1 & \boldsymbol{F}_y^- \end{bmatrix} \begin{bmatrix} \mathbf{A}'_1 \\ \mathbf{A}'_3 \end{bmatrix} \quad (24)$$

with

$$\mathbf{A}'_1 = (\sinh \boldsymbol{\Gamma}_z \bar{l}_z)^{-1} \mathbf{A}_1$$

and so on.

The scattering parameters are obtained by solving (21) or (24) for the outgoing wave vectors $\mathbf{B}_i$.

*E. Cascaded Junctions*

To demonstrate the approach, we consider a series connection of a general junction and a step discontinuity (Fig. 3). In the junction, the incoming wave $\mathbf{A}_2$ is unknown. We use the transmission matrix equation (19) for the general junction and additionally the transmission matrix equation for the step discontinuity [8] (15) in adapted form

$$\begin{bmatrix} \mathbf{A}_7 \\ \mathbf{0} \\ \hline \mathbf{B}_7 \end{bmatrix} = \left[\begin{array}{cc} \widetilde{\boldsymbol{T}}_+ & \widetilde{\boldsymbol{T}}_- \\ \boldsymbol{T}_2^c \boldsymbol{\Gamma}_2 & -\boldsymbol{T}_2^c \boldsymbol{\Gamma}_2 \\ \hline \widetilde{\boldsymbol{T}}_- & \widetilde{\boldsymbol{T}}_+ \end{array}\right] \begin{bmatrix} \boldsymbol{F}_+ \mathbf{A}_2 \\ \boldsymbol{F}_- \mathbf{B}_2 \end{bmatrix} \quad (25)$$

with the submatrices

$$\widetilde{\boldsymbol{T}}_{\pm} = \frac{1}{2}\,(\boldsymbol{T}_7^t \boldsymbol{T}_{2\to 7} \pm \boldsymbol{\Gamma}_7^{-1} \boldsymbol{T}_7^t \boldsymbol{T}_{2\to 7} \boldsymbol{\Gamma}_2). \quad (26)$$

$\boldsymbol{T}_2^c$ corresponds to the front plate of the step discontinuity and the propagation is given by the Fourier matrices $\boldsymbol{F}_{\pm} =$

$$\begin{aligned} \mathcal{T}_n^{\pm} &= \boldsymbol{T}_{y\to n}\,(\tanh \boldsymbol{\Gamma}_z \bar{l}_z)^{-1}\,\boldsymbol{R}_n \pm \boldsymbol{T}_n & (n &= 1,2) \\ \mathcal{T}_{mn} &= \boldsymbol{T}_{y\to m}\,(\sinh \boldsymbol{\Gamma}_z \bar{l}_z)^{-1}\,\boldsymbol{R}_n & (m,n &= 1,2) \\ \boldsymbol{W}_{mn} &= \mathcal{G}_{n\to m}\,(\sinh \boldsymbol{\Gamma}_z \bar{l}_z)^{-1}\,\boldsymbol{R}_n & (m &= 3,4;\ n = 1,2) \\ \boldsymbol{W}'_{mn} &= \mathcal{G}_{n\to m}\,\boldsymbol{V}_z\,(\sinh \boldsymbol{\Gamma}_z \bar{l}_z)^{-1}\,\boldsymbol{R}_n & (m &= 3,4;\ n = 1,2). \end{aligned} \quad (20)$$

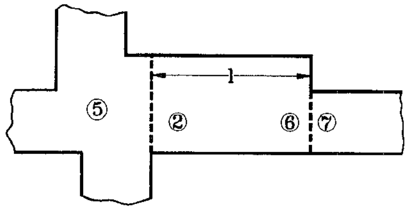


Fig. 3. Series connection of a general waveguide junction and a step discontinuity.

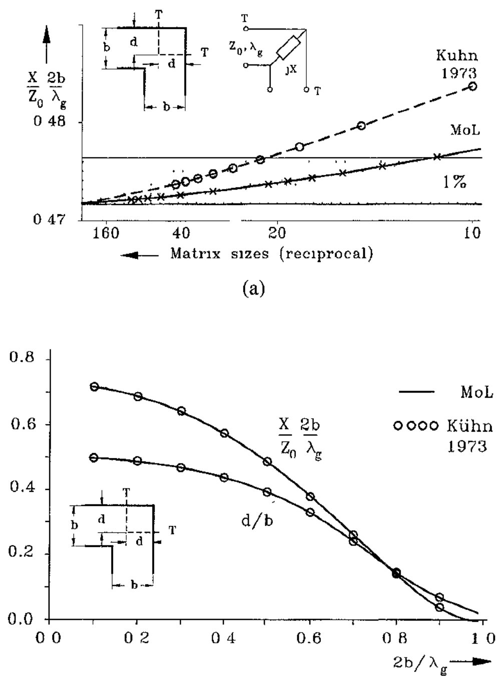


(b)

Fig. 4. Symmetric rectangular $E$-plane corner. (a) Convergence behavior of the normalized shunt reactance $X/Z_0 \cdot 2b/\lambda_g$ with respect to reciprocal matrix size. (b) Normalized shunt reactance $X/Z_0 \cdot 2b/\lambda_g$ and its location $d/b$ as a function of normalized frequency. ($\lambda_g$ guide wavelength, $Z_0$ characteristic impedance) o o o MMT [1].

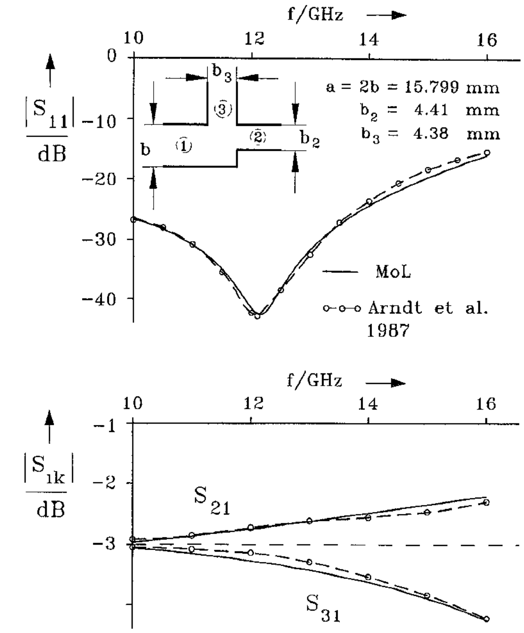


Fig. 5. Asymmetric $E$-plane T-junction. Magnitude of the scattering coefficients as a function of frequency o o o MMT [2].

$\exp(\pm \Gamma \bar{l})$ where $\bar{l}$ is the normalized distance between the junction and the step discontinuity. We eliminate $\mathbf{A}_2$ and solve for the outgoing wave coefficients $\mathbf{B}$ to compute the scattering matrix as above.

## III. Results

To verify the analysis of single and cascaded junctions, the scattering parameters or the resulting equivalent circuit parameters for two examplary structures have been computed and compared with results of the mode matching technique (MMT).

Fig. 4 shows the equivalent circuit parameters for a symmetric rectangular $E$-plane corner [1]. The equivalent circuit is valid for the fundamental mode only. The network parameters are computed from the scattering coefficients $S_{11}$ and $S_{21}$ by the following relations

$$jB_1 Z_0 = \frac{2}{1 + S_{11} + S_{21}} - 1$$
$$jB_2 Z_0 = \frac{2S_{21}}{(1 + S_{11})^2 - S_{21}^2} \qquad (27)$$

and

$$\frac{X}{Z_0} = -\left(2B_1 Z_0 + \frac{(B_1 Z_0)^2 + 1}{B_2 Z_0}\right)^{-1}$$
$$\frac{d}{b} = 1 + \frac{1}{\gamma_0 b} \tan^{-1}\left(B_1 Z_0 + 2B_2 Z_0\right)^{-1}. \qquad (28)$$

The guide wavelength runs $\lambda_g = 2\pi/\gamma_0 k_0$ and $Z_0$ is the characteristic impedance of the $H_{10}$ mode.

In Fig. 4(a) the convergence behavior of the normalized shunt reactance $X/Z_0 \cdot 2b/\lambda_g$ with respect to the reciprocal matrix sizes is given. As in the method of lines, not the whole system matrix in (24) must be inverted, but only two half-size matrices, the comparable matrix dimension is smaller for the same accuracy. In Fig. 4(b) the normalized shunt reactance and its location $d/b$ are presented as a function of normalized frequency. Both curves exactly coincide with the reference values.

As an example for cascaded discontinuities, the scattering coefficients of an asymmetric $E$-plane T-junction are presented in Fig. 5 as a function of frequency, which are also in very good agreement with MMT results [2].

## IV. Summary

For general junctions in rectangular waveguides the potential is computed on *two crossed line systems*. In the central (resonator) region it is represented by a superposition of two potentials with a one-dimensional discretization for each of them. They are evaluated by field matching at the terminals after suitable extrapolation to the boundaries of the respective line systems. Finally, matrix equations are derived for the incoming and outgoing waves to compute the scattering parameters. Cascaded junctions are easily analyzed by combining the matrix equations.

The scattering parameters for the asymmetric T-junction are in good agreement with literature. For the $E$-plane corner, the convergence of the MoL is better than for the mode matching technique with respect to the matrix sizes.

## APPENDIX

## EXTRAPOLATION OF THE POTENTIAL $\boldsymbol{\psi}_z$ TO $z = 0$ AND $z = l_z$

The potential in spatial domain

$$\boldsymbol{\psi}_z = \boldsymbol{T}_z \, \overline{\boldsymbol{\psi}}_z$$

is calculated by means of the transformation matrix

$$(\boldsymbol{T}_z)_{ik} = \sqrt{\frac{2-\delta_{0k}}{N_z}} \cos \frac{(i+\frac{1}{2})k\pi}{N_z} \qquad (k = 0 \ldots N_z - 1)$$

on the lines $z = (i + \frac{1}{2})\mathrm{h}_z$ giving

$$\psi_z(z) = \sum_{k=0}^{N_z-1} \sqrt{\frac{2-\delta_{0k}}{N_z}} \cos\left(\frac{k\pi}{l_z} z\right) \overline{\psi}_{zk}. \tag{29}$$

We extrapolate this formula to $z = 0$, where the cosine terms become 1.

After discretization in $y$ direction we obtain

$$\psi_{zi} = \sum_{k=0}^{N_z-1} \sqrt{\frac{2-\delta_{0k}}{N_z}} \Big(\exp\left(-\gamma_{yk}\overline{y}_i\right) A_{zk} + \exp\left(\gamma_{yk}\overline{y}_i\right) B_{zk}\Big)$$
$$(i = 0 \ldots N_y - 1) \tag{30}$$

with $\overline{y}_i = (i + \frac{1}{2})\overline{\mathrm{h}}_y$.

At the extrapolation to $z = l_z$, the cosine terms in (29) become $(-)^k$; hence, at this position (30) is valid with this additional sign. Using (30), we finally obtain (9) and (12) with (10).

## REFERENCES


[1] E. Kühn, "A mode-matching method for solving field problems in waveguide and resonator circuits," *Arch. Elektron. Uebertragungstech., AEÜ 27*, pp. 511–518, 1973.

[2] F. Arndt *et al.*, "Optimized $E$-plane T-junction series power dividers," *IEEE Trans. Microwave Theory Tech., MTT–35* (11), pp. 1052–1059, 1987.

[3] R. Mittra and W. W. Lee, *Analytical Techniques in the Theory of Guided Waves.* New York: Macmillan, 1971.

[4] U. Schulz and R. Pregla, "A new technique for the analysis of the dispersion characteristics of planar waveguides," *Arch. Elektron. Übertragungstech., AEÜ 34*, pp. 169–173, 1980.

[5] U. Schulz, "The Method of Lines—A New Technique for the Analysis of Planar Microwave Structures" (in German), Ph.D. dissertation, Fern Univ., Hagen, Federal Republic of Germany, 1980.

[6] R. Pregla and W. Pascher, "The Method of Lines," in *Numerical Techniques for Microwave and Millimeter Wave Passive Structures*, T. Itoh, Ed. New York: Wiley, 1989, pp. 381–446.

[7] U. Schulz, "Evaluation of the equivalent circuit parameters of posts and diaphragms in waveguides by the method of lines" (in German), *Arch. Elektron. Übertragungstech., AEÜ 39*, pp. 203–207, 1985.

[8] W. Pascher and R. Pregla, "Analysis of rectangular waveguide discontinuities by the method of lines," *IEEE Trans. Microwave Theory Tech., MTT-43*, pp. 416–420, Feb. 1995.

[9] R. Pregla, "Analysis of a bend discontinuity by the method of lines," *Frequenz* (Germany), vol. 45, pp. 213–216, 1991.



**Wilfrid Pascher** (M'94) was born in Graz, Austria, on September 17, 1958. He received the master's degree in technical physics (Dipl.-Ing.) from the Technical University Graz and the doctorate of engineering (Dr.-Ing.) from the FernUniversität in Hagen, in 1984 and 1990, respectively.

From 1985 to 1990 he was a Research Assistant in the Department of Electrical Engineering of the FernUniversität, where he was engaged in the investigation of planar and rectangular waveguide components. Since 1990, he has been a Senior Engineer and is currently involved in waveguide theory and the numerical modelling of passive components for microwaves and integrated optics.

**Reinhold Pregla** (M'76–SM'83) received the master's degree in electrical engineering (Dipl. Ing.) and the doctorate engineering (Dr. Ing.) from the Technische Universitt Braunschweig, West Germany, in 1963 and 1966, respectively.

From 1966 to 1969 he was a Research Assistant in the Department of Electrical Engineering of the Technische Universitt Braunschweig (Institut fr Hochfrequenztechnik), where he was engaged in investigations of microwave filters. After the Habilitation, he was a Lecturer in high frequencies at the Technische Universitt Braunschweig. Since 1973 he has held the position of Professor at the Ruhr-Universitt Bochum, West Germany, and since 1975, he has held the position of full Professor in Electrical Engineering at the FernUniversität (a university for distance study) in Hagen, West Germany. His fields of investigation include microwave passive circuits, waveguide theory for microwaves and optics, antennas and laser modelling.